Research Square

Preprints are preliminary reports that have not undergone peer review.
They should not be considered conclusive, used to inform clinical practice,
or referenced by the media as validated information.

Targeting KPNA2 Enhances Bortezomib Anti-myeloma activity Through Suppressing Non-Canonical NF-κB-Mediated Autophagy in Multiple Myeloma

huan wang
First Affiliated Hospital of Nanchang University
Lifang zou
First Affiliated Hospital of Nanchang University
Zhiwei Chen
First Affiliated Hospital of Nanchang University
Meng Chen
First Affiliated Hospital of Nanchang University
Wan Zhang
First Affiliated Hospital of Nanchang University
Lugui Qiu
Chinese Academy of Medical Sciences & Peking Union Medical College
Fei Li
ndyfy01238@ncu.edu.cn

First Affiliated Hospital of Nanchang University

Research Article

Keywords: multiple myeloma, autophagy, KPNA2, bortezomib, NF-κB

Posted Date: September 29th, 2026

DOI: https://doi.org/10.21203/rs.3.rs-10959728/v1

License: This work is licensed under a Creative Commons Attribution 4.0 International License.
Read Full License

Additional Declarations: No competing interests reported.

Abstract

Bortezomib (BTZ)-based therapy has substantially improved clinical outcomes in multiple myeloma (MM), the emergence of BTZ resistance remains a major obstacle to achieving durable disease control. Although autophagy-mediated proteotoxic stress adaptation has been implicated in modulating cellular responses to BTZ, the upstream regulators that orchestrate this adaptive process and their contribution to BTZ sensitivity remain poorly understood. In this study, we identify karyopherin α2 (KPNA2), a critical nucleocytoplasmic transport receptor, as a previously unrecognized regulator of BTZ sensitivity in MM. Integrated analysis of public datasets and clinical samples demonstrated that KPNA2 expression is significantly elevated during MM progression and independently predicts inferior survival. Functional investigations revealed that KPNA2 promotes MM cell proliferation and resistance to BTZ-induced apoptosis. Mechanistically, KPNA2 selectively activates the non-canonical NF-κB pathway, promoting p100 processing and nuclear accumulation of p52/RelB, which subsequently enhances autophagic activity and establishes a protective stress-adaptation program. Genetic depletion or pharmacological inhibition of KPNA2 suppresses this signaling cascade, inhibits autophagy, and enhances BTZ sensitivity *in vitro* and *in vivo*. Collectively, our findings establish KPNA2 as a molecular bridge linking nuclear transport machinery with alternative NF-κB signaling and autophagy-dependent proteostasis. Targeting the KPNA2/non-canonical NF-κB/autophagy axis represents a promising therapeutic strategy for enhancing BTZ sensitivity and treatment responses in MM.

Introduction

Multiple myeloma (MM) is an incurable plasma cell malignancy characterized by uncontrolled expansion of clonal plasma cells in the bone marrow [1]. Although the introduction of proteasome inhibitors (PIs), immunomodulatory agents, and monoclonal antibodies has substantially improved patient outcomes, relapse and variability in therapeutic response remain major clinical challenges [2]. Bortezomib (BTZ), the first clinically approved proteasome inhibitor, is a cornerstone therapy for MM. By blocking proteasomal degradation, BTZ induces accumulation of misfolded proteins, endoplasmic reticulum stress, and apoptotic cell death [3]. However, prolonged BTZ exposure promotes adaptive responses that enable myeloma cells to maintain proteostasis and survive therapeutic stress.

Autophagy has emerged as a critical adaptive mechanism that reduces BTZ sensitivity in MM [4–6]. As a conserved lysosome-dependent degradation pathway, autophagy eliminates damaged organelles and aggregated proteins to maintain cellular homeostasis [7]. Given the high proteotoxic burden of plasma cells, autophagy provides a compensatory mechanism that alleviates BTZ-induced proteotoxic stress and promotes malignant cell survival [8]. Previous studies have demonstrated that pharmacological or genetic inhibition of autophagy enhances BTZ sensitivity in MM cells, highlighting autophagy as a potential therapeutic target [8–10]. However, the upstream regulators responsible for activating autophagy-mediated survival adaptation during BTZ treatment remain largely unknown.

Karyopherin α2 (KPNA2, also known as importin α2) is a key component of the classical nuclear transport system that mediates the intracellular trafficking of proteins containing nuclear localization signals (NLSs) between the cytoplasm and nucleus [11]. Although initially characterized as a transport adaptor, accumulating evidence indicates that KPNA2 has broader biological functions in cancer development by regulating the localization and activity of transcriptional regulators involved in proliferation, stemness, DNA damage response, and tumor progression [12]. Aberrant KPNA2 expression has been reported in multiple malignancies and is frequently associated with aggressive disease characteristics and unfavorable clinical outcomes [13–15]. In addition, emerging studies suggest that KPNA2 may participate in oncogenic signaling networks beyond its canonical transport function [12]. However, whether KPNA2 modulates BTZ sensitivity in MM, particularly through regulation of stress-adaptive pathways that enable malignant plasma cells to tolerate proteotoxic stress, remains largely unknown.

NF-κB signaling plays an essential role in MM pathogenesis, disease progression, and therapeutic resistance [16–18]. Although canonical NF-κB activation mediated by p65/p50 has been extensively investigated in MM, the contribution of the non-canonical pathway characterized by p100 processing and p52/RelB activation to BTZ resistance remains less well defined [18]. Increasing evidence indicates that NF-κB signaling not only promotes malignant cell survival but also participates in cellular stress adaptation by regulating processes such as autophagy [19–21]. KPNA2, a key regulator involved in nucleocytoplasmic transport, has been implicated in multiple oncogenic signaling networks, and previous studies have suggested a potential association between KPNA2 expression and NF-κB activity in cancer contexts [22]. However, whether KPNA2 is involved in regulating NF-κB-dependent stress responses and drug sensitivity in MM remains largely unknown.

In this study, we demonstrate that KPNA2 is significantly upregulated in MM and independently predicts unfavorable clinical outcomes. Mechanistically, KPNA2 selectively activates the non-canonical NF-κB pathway to promote nuclear accumulation of p52/RelB and trigger autophagy-dependent stress adaptation, thereby reducing BTZ sensitivity in MM cells. Our findings identify KPNA2 as a critical molecular link between nuclear transport regulation and BTZ sensitivity, providing a potential therapeutic strategy for improving BTZ efficacy in MM.

Materials and methods

Clinical samples

Bone marrow specimens were obtained from healthy donors (HD, n = 6) and newly diagnosed multiple myeloma (NDMM) patients (n = 13) at the First Affiliated Hospital of Nanchang University. The diagnosis of MM was based on the International Myeloma Working Group (IMWG) consensus criteria [23]. Monocytes were first isolated from fresh bone marrow specimens (10 mL) using lymphocyte separation medium (Solarbio, Beijing, China, Cat# P8900), followed by $CD138^+$ cell selection with CD138 antibody-conjugated magnetic beads (Miltenyi, Bergisch Gladbach, Germany, Cat# 130-051-301). This study was

approved by the Ethics Committee of the First Affiliated Hospital of Nanchang University in accordance with the Declaration of Helsinki. Written informed consent was obtained from all individual participants.

Cell culture

Human MM cell lines (RPMI 8226, ARP1, U266, MM1.S, and H929) were maintained in RPMI 1640 medium (Solarbio, Beijing, China, Cat# 11875) supplemented with 10% fetal bovine serum (CellMax, Beijing, China, Cat# SA102) and 1% penicillin/streptomycin (Solarbio, Beijing, China, Cat# P1400) at 37°C in a 5% CO_2 atmosphere. HEK293T cells were cultured under the same conditions in DMEM (Solarbio, Beijing, China, Cat# 11995) with 10% fetal bovine serum and 1% penicillin/streptomycin.

Cell viability

Cell proliferation was assessed daily for 4 days using the Cell Counting Kit–8 (CCK–8) (Beyotime, Shanghai, China, Cat# C0037) in 96-well plates. Absorbance at 450 nm was measured using a microplate reader (Thermo Fisher Scientific).

Reagents and antibodies

Ivermectin (HY-15310), chloroquine (HY-17589A), and bortezomib (HY-10227) were purchased from MedChemExpress (NJ, USA). SN52 was obtained from Selleck Chemicals (TX, USA, Cat# P1238). Antibodies against PARP-1 (#9542S), Caspase-3 (#9661S), LC3 (#2775S), p65 (#8242S), and p-p65 (#3033S) were sourced from Cell Signaling Technology (MA, USA). Antibodies against KPNA2 (10819-1-AP), Beclin-1 (11306-1-AP), and β-actin (66009-1-Ig) were purchased from Proteintech (Wuhan, China). Antibodies targeting ULK1 (HY-P80366), p-ULK1 (HY-P81065), Atg5 (HY-P80022), Atg13 (HY-P81905), FIP200 (HY-P80130), p100 (HY-P80763), RelB (HY-P80306), and p105/p50 (HY-P80244) were obtained from MedChemExpress (NJ, USA). The antibody against p52 (YC0200) was purchased from Immunoway (TX, USA).

Plasmids and virus production

Empty vector (EV) and shRNA plasmids were purchased from Tsingke Technology (Changsha, China). For KPNA2 overexpression, the full-length coding sequence of KPNA2 was inserted into the pLV-Puro-CMV vector. Endotoxin-free, transfection-grade plasmid DNA was amplified in *E. coli* DH5α competent cells (TransGen Biotech, Beijing, China, Cat# CD521-01) and purified using the EndoFree Midi Plasmid Kit (TIANGEN, Beijing, China). Lentiviruses were generated by co-transfecting HEK293T cells with psPAX2, pMD2.G, and the corresponding recombinant plasmid using Lipofectamine 3000 (Invitrogen, USA). Viral supernatants were harvested at 48 or 72 h after transfection and concentrated by ultracentrifugation (20,000×*g*, 2.5 h, 4°C). Cells were transduced with concentrated lentivirus in the presence of 8 μg/mL

polybrene and selected with puromycin (Solarbio, Beijing, China) beginning 72 h after transduction to establish stable cell lines. KPNA2 overexpression or knockdown efficiency was confirmed by RT–qPCR and western blotting. The shRNA sequences are listed below: KPNA2-shRNA-1 (5'-CTACCTCTGAAGGCTACACTT-3'), KPNA2-shRNA-2 (5'-TCATGTAGCTGAGACATAAAT-3').

Western blotting

After culture under the indicated experimental conditions, cells were harvested, washed with cold PBS, and lysed in RIPA strong buffer (Solarbio, Beijing, China, Cat# R0010) containing protease inhibitors. Nuclear and cytoplasmic fractions were prepared using a Nuclear and Cytoplasmic Protein Extraction Kit (Beyotime, Shanghai, China, Cat# P0028) according to the manufacturer's instructions. Total protein concentrations were determined using a BCA Protein Assay Kit (Beyotime, Shanghai, China, Cat# P0012). Protein samples (10–30 μg) were separated by SDS-PAGE and transferred to PVDF membranes (Merck Millipore, Germany, Cat# IPVH00010). Membranes were blocked with 5% skim milk in TBST and incubated with primary antibodies overnight at 4°C. Primary antibodies used were against KPNA2, PARP-1, Caspase-3, LC3, ULK1, p-ULK1, Atg5, Atg13, FIP200, p100, p52, RelB, p65, p-p65, p105/p50, and Beclin-1 (all at 1:1000 dilution), and β-actin (1:10,000 dilution). After three washes with TBST for 10 min each, the membranes were incubated with the appropriate secondary antibodies for 1–2 h at room temperature. Goat anti-rabbit IgG secondary antibody (1:3000) was used for KPNA2, PARP-1, Caspase-3, LC3, ULK1, p-ULK1, Atg5, Atg13, p100, p52, RelB, p65, p-p65, and p105/p50; whereas goat anti-mouse IgG secondary antibody was used for FIP200 (1:3000) and β-actin (1:10,000). The membranes were then washed three times with TBST for 10 min each, incubated with enhanced chemiluminescence detection reagents (Proteintech, Wuhan, China, Cat# PK10002) for 1 min, and visualized using a ChemiDoc XRS chemiluminescence imaging system (Bio-Rad).

Transmission Electron Microscopy (TEM)

MM cells were collected by centrifugation, fixed in 2.5% glutaraldehyde in 0.1 M cacodylate buffer (pH 7.4) at 4°C for 3 h, rinsed with the same buffer, post-fixed in 1% osmium tetroxide (OsO_4), dehydrated through a graded ethanol series, and embedded in Epon 812. Ultrathin sections were stained with 2% uranyl acetate and lead citrate, and subsequently examined using a TECNAI G2 20 TWIN electron microscope (FEI, Eindhoven, The Netherlands).

Quantitative real-time PCR

Total RNA was extracted using TRIzol (Invitrogen) and reverse-transcribed with a cDNA reverse transcription kit (TransGen Biotech, Beijing, China, Cat# AT341-01). RT–qPCR was performed in triplicate using SYBR Green Master Mix (ABclonal, Wuhan, China, Cat# RK21203) on a StepOnePlus Real-Time PCR System (Thermo Fisher Scientific). The expression level of the target gene was normalized to ACTIN, and data were analyzed using the $2^{-}\Delta\Delta Ct$ method. Primers were synthesized by Sangon Biotech

(Shanghai, China), with the following sequences: ACTIN (forward primer: 5'-CATGTACGTTGCTATCCAGGC-3'; reverse primer: 5'- CTCCTTAATGTCACGCACGAT-3'), KPNA2 (forward primer: 5'-CTGCCCGTCTTCACAGATTCA- 3', reverse primer: 5'-GCGGAGAAGTAGCATCATCAGG- 3').

Flow cytometry

Cell apoptosis was assessed using the APC-Annexin V/PI Apoptosis Detection Kit (Lianke Biotech, Hangzhou, China, Cat# AP107) according to the manufacturer's instructions. Briefly, cells were harvested by centrifugation, washed with cold PBS, and resuspended in binding buffer. The cells were then stained with Annexin V and propidium iodide (PI) to identify viable, early apoptotic, late apoptotic dead cells, respectively. Stained cells were then analyzed using a DxFLEX flow cytometer (Beckman Coulter, CA, USA).

Tumor xenograft model

Female BALB/c nude mice (4–5 weeks old, approximately 20 g) were obtained from Jiangsu GemPharmatech Co., Ltd. and housed under specific pathogen-free (SPF) conditions at the Laboratory Animal Center of our hospital. After expansion, myeloma cells were resuspended in sterile PBS and mixed with Matrigel (1:1). A total of 5×10^6 cells in 200 μL suspension were subcutaneously injected into the axillary region of each mouse. Seven days after inoculation, mice were randomly divided into indicated treatment groups and intraperitoneally administered bortezomib (BTZ, 0.5 mg/kg), ivermectin (IVM, 2 mg/kg), or vehicle control twice weekly for 4 weeks. Tumor size was measured every 5 days, and tumor volume was calculated using the formula: $V = (D \times d^2)/2$, where D represents the longest diameter and d represents the shortest diameter. After 30 days, mice were euthanized, and tumors were collected, photographed, and weighed. All animal experiments were approved by the Laboratory Animal Welfare and Ethics Committee of the First Affiliated Hospital of Nanchang University and performed in accordance with institutional guidelines for animal care and use.

Statistical analysis

Survival differences between subgroups were analyzed using the Kaplan–Meier method with log-rank tests. Overall survival (OS) was defined as the time from treatment initiation to death from any cause or the last known date the patient was alive. All experiments were performed at least three times. For comparisons between two independent groups, an unpaired, two-tailed Student's t-test was applied. For comparisons involving three or more groups, one-way or two-way analysis of variance (ANOVA) was used, followed by Tukey's or Bonferroni's post-hoc test for multiple comparisons. Graphs were generated with GraphPad Prism 8 software (GraphPad Software, Inc., La Jolla, CA, USA). $p < 0.05$ was considered to possess a statistically significant difference. * $p < 0.05$; ** $p < 0.01$; *** $p < 0.001$.

Results

KPNA2 is progressively upregulated during MM progression and independently predicts poor clinical outcomes

To identify novel molecular determinants associated with MM progression and therapeutic resistance, we first performed integrated transcriptomic analyses using two independent GEO datasets (GSE47552 and GSE16122). Differential expression analysis between normal plasma cells and MM samples identified 53 overlapping genes, among which KPNA2 attracted our attention due to its previously reported involvement in nuclear transport regulation and malignant progression **(**Fig. 1A **and Supplementary Fig. 1)**. Consistent with the bioinformatic screening results, KPNA2 expression displayed a progressive elevation during disease evolution. In the GSE47552 cohort, KPNA2 levels were significantly increased in monoclonal gammopathy of undetermined significance (MGUS), smoldering multiple myeloma (SMM), and overt MM compared with healthy controls **(**Fig. 1B**)**, indicating that KPNA2 upregulation occurs early during plasma cell transformation and persists during malignant progression.

Validation using the independent GSE16122 cohort further confirmed that KPNA2 expression was markedly elevated in MM and plasma cell leukemia (PCL) compared with normal plasma cells **(**Fig. 1C**)**. Importantly, survival analysis demonstrated that patients with high KPNA2 expression exhibited significantly inferior OS compared with those with low KPNA2 expression in large independent cohorts **(**Fig. 1D, E**)**. Clinical validation using bone marrow plasma cells from MM patients further confirmed KPNA2 overexpression compared with healthy donors **(**Fig. 1F, G**)**. In addition, analysis of BTZ-treated patients revealed significantly higher KPNA2 expression in patients with progressive disease (PD) than in patients achieving complete response (CR) or better **(**Fig. 1H**)**.

The GSE24080 cohort was further used to analyze the clinical relevance of KPNA2. High KPNA2 expression was significantly correlated with elevated lactate dehydrogenase (LDH) ($p = 0.002$), international staging system stage III (ISS III) ($p = 0.011$), serum β2-microglobulin ≥ 5.5 mg/L ($p = 0.011$), and cytogenetic abnormalities ($p = 0.007$) **(Supplementary Table 1)**. Univariate and multivariate Cox regression analyses incorporating KPNA2, age ≥ 65, elevated LDH, renal dysfunction, anemia, serum β2-microglobulin, albumin, and cytogenetic abnormalities demonstrated that high KPNA2 expression served as an independent adverse prognostic factor for MM OS ($p = 0.032$; hazard ratio [HR] = 1.422; 95% confidence interval [CI]: 1.031–1.962) **(Supplementary Table 2)**. Collectively, these findings indicate that KPNA2 is significantly upregulated in MM and correlates with poor clinical prognosis.

KPNA2 facilitates malignant progression and decreases BTZ sensitivity in MM cells

To investigate the biological function of KPNA2 in MM, we generated stable KPNA2 knockdown models in RPMI-8226 and H929 cells using two independent shRNAs. Efficient depletion of KPNA2 expression was confirmed by immunoblotting **(**Fig. 2A, B**)**. Functional assays revealed that KPNA2 silencing significantly inhibited MM cell proliferation and reduced cellular viability **(**Fig. 2C**)**. Mechanistically,

KPNA2 depletion increased apoptotic susceptibility, as demonstrated by enhanced cleavage of caspase-3 and a substantial increase in Annexin V-positive apoptotic cells (Fig. 2D **and Supplementary Fig. 2A)**. Conversely, ectopic KPNA2 overexpression in H929 and ARP1 cells produced the opposite phenotype (Fig. 2E, F). KPNA2-overexpressing (OE) cells displayed enhanced proliferation and reduced sensitivity to apoptotic induction (Fig. 2G).

When exposed to increasing concentrations of BTZ, KPNA2-overexpressing cells maintained significantly higher viability than control cells (Fig. 2H). Flow cytometric analysis further demonstrated reduced BTZ-induced apoptosis in KPNA2-overexpressing cells **(Supplementary Fig. 2B)**. Collectively, these findings establish KPNA2 as a functional driver of malignant progression of MM cells.

KPNA2 promotes autophagic stress adaptation in MM cells

Because autophagy represents an important survival mechanism allowing MM cells to tolerate proteotoxic stress induced by proteasome inhibition [4–6], we investigated whether KPNA2 regulates autophagic responses. RNA sequencing analysis performed after KPNA2 depletion revealed significant enrichment of autophagy-related signaling pathways, suggesting a potential connection between KPNA2 and autophagic regulation **(Supplementary Fig. 3A, B)**.

Subsequent experimental validation demonstrated that KPNA2 positively regulated autophagic activity. KPNA2 knockdown resulted in reduced LC3-II accumulation, whereas KPNA2 overexpression increased LC3-II levels in MM cells (Fig. 3A, B). Transmission electron microscopy provided additional ultrastructural evidence, showing decreased autophagosome and autolysosome formation following KPNA2 depletion and increased autophagic structures after KPNA2 overexpression (Fig. 3C, D, E).

Consistently, KPNA2 regulated multiple components of the autophagy initiation machinery, including phosphorylated ULK1, ULK1, Beclin-1, FIP200, ATG13, and ATG5 (Fig. 3F). Pharmacological inhibition of KPNA2 activity using ivermectin reduced expression of autophagy-associated proteins in a dose-dependent manner, further supporting a regulatory role for KPNA2 in autophagic activation (Fig. 3G). Together, these results indicate that KPNA2 acts as a positive regulator of autophagic activation and may facilitate autophagic stress adaptation in MM cells.

KPNA2-mediated autophagic stress adaptation attenuates BTZ sensitivity

Since autophagy represents a major adaptive mechanism that enables tumor cells to survive proteasome inhibition, we next asked whether KPNA2-mediated autophagy functionally modulates tumor cell sensitivity to BTZ. KPNA2-overexpressing MM cells were treated with BTZ alone or in combination with chloroquine, which inhibits autophagic degradation by blocking lysosomal acidification. Although KPNA2 overexpression conferred a survival advantage upon BTZ treatment, concomitant inhibition of autophagy with chloroquine markedly weakened this protective effect. Specifically, combined BTZ and chloroquine treatment resulted in a greater reduction in cell viability than

BTZ monotherapy, indicating that blockade of autophagy restored BTZ sensitivity in KPNA2-overexpressing cells (Fig. 4A).

Consistent with this effect, immunoblot analysis showed that inhibition of autophagy enhanced BTZ-induced apoptotic signaling in KPNA2-overexpressing MM cells. Compared with BTZ treatment alone, the combination of BTZ and chloroquine led to increased expression of apoptotic markers, including cleaved PARP-1 and cleaved caspase-3, indicating stronger activation of the apoptotic cascade upon autophagy blockade **(Supplementary Fig. 4A)**.

Flow cytometric analysis further confirmed that chloroquine significantly enhanced BTZ-induced apoptosis in KPNA2-overexpressing MM cells. The proportion of apoptotic cells was markedly increased in the combination treatment group compared with the BTZ-alone group (Fig. 4B, C), suggesting that autophagy inhibition converts the KPNA2-associated survival advantage into increased susceptibility to BTZ-induced cell death. These findings indicate that autophagy acts as an important downstream survival mechanism of KPNA2 under proteasome-inhibitory stress.

KPNA2 selectively activates the non-canonical NF-κB pathway to promote p52/RelB nuclear accumulation and autophagic adaptation

To further elucidate the upstream signaling mechanisms responsible for KPNA2-mediated autophagy activation, we investigated whether NF-κB signaling contributes to this regulatory process. NF-κB is a well-established regulator of MM pathogenesis and plays an important role in malignant cell survival, stress adaptation, and therapeutic resistance [16–18]. Given the ability of NF-κB signaling to regulate cellular responses to proteotoxic stress, we examined whether KPNA2 influences NF-κB pathway activation in MM cells. Interestingly, modulation of KPNA2 expression had minimal effects on the canonical NF-κB pathway. Specifically, the protein levels of canonical NF-κB components, including p65, phosphorylated p65, p105, and p50, remained largely unchanged following KPNA2 knockdown or overexpression. In contrast, KPNA2 exhibited a selective regulatory effect on the non-canonical NF-κB pathway. KPNA2 depletion markedly decreased the expression of key components of the alternative NF-κB pathway, including p100, p52, and RelB, in RPMI-8226 and H929 cells. Conversely, ectopic KPNA2 overexpression significantly increased the abundance of p100, p52, and RelB in H929 and ARP1 cells (Fig. 5A). These findings indicate that KPNA2 preferentially regulates non-canonical rather than canonical NF-κB signaling in MM cells.

To further validate the regulatory relationship between KPNA2 and non-canonical NF-κB activation, KPNA2-overexpressing MM cells were treated with ivermectin, a pharmacological inhibitor associated with KPNA2-mediated nuclear transport activity [24, 25]. Ivermectin treatment substantially reduced the expression of p100, p52, and RelB, suggesting that KPNA2 activity is required for maintaining non-canonical NF-κB pathway activation (Fig. 5B). Furthermore, inhibition of the non-canonical NF-κB pathway using SN52 significantly decreased the expression of autophagy-associated proteins, including

LC3-II and other key autophagic regulators, in KPNA2-overexpressing cells (Fig. 5C). These results demonstrate that non-canonical NF-κB signaling functions downstream of KPNA2 and contributes to KPNA2-mediated autophagic regulation.

Because activation of the non-canonical NF-κB pathway relies on the nuclear translocation of p52/RelB transcriptional complexes, we next examined whether KPNA2 affects their subcellular localization. Nuclear and cytoplasmic protein fractionation assays revealed that KPNA2 depletion significantly reduced nuclear accumulation of p52 and RelB, whereas KPNA2 overexpression markedly enhanced their nuclear localization (Fig. 5D). These findings suggest that KPNA2 facilitates activation of p52/RelB-dependent transcriptional programs in MM cells. Collectively, our data identify KPNA2 as an upstream regulator of non-canonical NF-κB signaling that promotes p52/RelB nuclear accumulation, enhances autophagic adaptation, and reduces BTZ sensitivity in MM.

KPNA2 inhibition restores BTZ sensitivity and enhances anti-myeloma efficacy in vitro and in vivo

Given the critical role of KPNA2 in mediating autophagic adaptation and reducing BTZ sensitivity, we next investigated whether targeting KPNA2 could restore BTZ responsiveness and improve therapeutic efficacy. We evaluated the anti-myeloma effects of pharmacological KPNA2 inhibition using ivermectin (IVM), either alone or in combination with BTZ in MM cells. Treatment with IVM alone significantly reduced the viability of RPMI-8226 and H929 cells and induced apoptotic cell death, indicating that KPNA2 inhibition itself exerts anti-myeloma activity. Importantly, combined treatment with IVM and BTZ produced a markedly stronger inhibitory effect compared with either single-agent treatment (Fig. 6A). The enhanced cytotoxicity was further confirmed by flow cytometric analysis, which demonstrated a substantial increase in Annexin V-positive apoptotic cells following combined KPNA2 inhibition and BTZ treatment **(Supplementary Fig. 6A)**. These findings indicate that pharmacological inhibition of KPNA2 effectively enhances the susceptibility of MM cells to BTZ-induced apoptosis.

To further determine whether KPNA2 inhibition improves BTZ efficacy *in vivo*, we established xenograft models using KPNA2-depleted RPMI-8226 cells and H929-derived tumors treated with IVM. Compared with control groups, genetic depletion or pharmacological inhibition of KPNA2 significantly delayed tumor growth, suggesting that KPNA2 is required for efficient MM tumor maintenance (Fig. 6B). Notably, combination therapy with KPNA2 inhibition and BTZ resulted in the most pronounced suppression of tumor progression, with significantly reduced tumor volumes and tumor weights compared with BTZ monotherapy (Fig. 6C, D).

Consistent with the *in vitro* findings, these *in vivo* results demonstrate that targeting KPNA2 enhances the anti-tumor activity of BTZ and improves BTZ responsiveness in MM cells. Collectively, our data establish KPNA2 inhibition as a promising therapeutic strategy to restore BTZ sensitivity and improve the efficacy of BTZ-based treatment in MM.

Discussion

Diminished sensitivity to BTZ remains a major obstacle to the long-term efficacy of BTZ-based therapy in MM. Although proteasome inhibitors have substantially improved patient survival, many patients eventually relapse as malignant plasma cells acquire adaptive survival mechanisms that reduce their responsiveness to BTZ [26, 27]. Previous studies have shown that diminished sensitivity to BTZ arises from multiple factors, including alterations in proteasome composition and activity, activation of unfolded protein response pathways, metabolic adaptation, changes in the tumor microenvironment, and enhanced autophagic activity [28–31]. These mechanisms collectively enable myeloma cells to tolerate sustained proteotoxic stress induced by proteasome inhibition. However, despite extensive investigation of downstream factors affecting therapeutic response, the upstream regulatory factors that coordinate adaptive survival programs and thereby determine cellular sensitivity to BTZ remain incompletely understood. Identifying such regulatory nodes is critical for understanding the molecular determinants of BTZ sensitivity and developing strategies to improve the efficacy of BTZ-based treatment.

In this study, we identify KPNA2 as a previously unrecognized molecular determinant of MM progression and BTZ sensitivity. Although KPNA2 has been reported as a cancer-associated factor in multiple malignancies [12–15], its functional significance in regulating BTZ sensitivity in MM has not been established. Our clinical and functional analyses demonstrate that KPNA2 is not merely a prognostic biomarker associated with aggressive disease features, but rather acts as an active driver of malignant progression and therapeutic adaptation. KPNA2 expression is progressively increased during MM development, from early plasma cell disorders to overt MM, and elevated KPNA2 levels are associated with unfavorable clinical characteristics and reduced OS. Moreover, increased KPNA2 expression in patients with progressive disease following BTZ treatment further supports its association with reduced BTZ sensitivity. These findings expand the current understanding of KPNA2 biology by demonstrating that KPNA2 contributes to disease aggressiveness and drug response regulation in MM.

A major conceptual advance of this study is the identification of KPNA2 as an upstream regulator of autophagy-mediated BTZ sensitivity. Autophagy has traditionally been considered a downstream adaptive response activated after exposure to cellular stress, particularly under conditions of proteotoxic injury caused by proteasome inhibition [32, 33]. In MM cells, which are highly dependent on protein synthesis and quality-control systems due to their immunoglobulin-producing phenotype, autophagy provides an essential compensatory mechanism to maintain intracellular homeostasis [34, 35]. Our findings demonstrate that KPNA2 positively regulates autophagic activity by modulating multiple components involved in autophagy initiation and progression, including ULK1, FIP200, ATG13, ATG5, Beclin-1, and LC3-II. Importantly, inhibition of autophagy markedly restored BTZ sensitivity in KPNA2-overexpressing cells, indicating that KPNA2-mediated autophagy is not merely associated with reduced BTZ sensitivity but functionally contributes to the enhanced survival of myeloma cells under BTZ treatment. Therefore, our study places KPNA2 upstream of the autophagic stress response and identifies a previously unrecognized regulatory mechanism controlling proteostasis adaptation during proteasome inhibition.

Mechanistically, our study reveals that KPNA2 reduces BTZ sensitivity through selective activation of the non-canonical NF-κB signaling pathway. NF-κB activation has long been recognized as a critical driver of MM pathogenesis, survival, and treatment resistance [36, 37]. However, previous investigations have predominantly focused on the canonical pathway involving p65/RelA and p50 activation, whereas the contribution of the alternative NF-κB pathway to BTZ sensitivity remains less well characterized. Here, we demonstrate that KPNA2 selectively regulates the non-canonical NF-κB pathway, as evidenced by changes in p100, p52, and RelB expression, while canonical NF-κB components including p65, phosphorylated p65, p105, and p50 remain largely unaffected. Furthermore, our nuclear fractionation studies reveal that KPNA2 promotes the nuclear accumulation of p52 and RelB, supporting enhanced activation of p52/RelB-dependent transcriptional programs. Pharmacological inhibition of non-canonical NF-κB signaling suppresses KPNA2-induced autophagic activation, establishing a functional link between KPNA2, alternative NF-κB signaling, and autophagy. These findings provide new insight into how selective activation of non-canonical NF-κB signaling contributes to stress adaptation and therapeutic resistance in MM.

The identification of the KPNA2/non-canonical NF-κB/autophagy axis also provides important therapeutic implications. Current treatment options for relapsed or refractory MM remain limited, largely due to the development of acquired resistance to previously effective agents. Our findings demonstrate that genetic depletion or pharmacological inhibition of KPNA2 enhances BTZ-induced apoptosis and significantly improves anti-myeloma efficacy both *in vitro* and *in vivo*. These results suggest that targeting KPNA2 may represent a rational strategy to resensitize resistant myeloma cells to proteasome inhibition. Importantly, rather than directly targeting BTZ-induced cytotoxic mechanisms, KPNA2 inhibition disrupts the adaptive survival network that allows malignant cells to tolerate proteotoxic stress. Therefore, combining KPNA2-targeting approaches with BTZ may provide a complementary therapeutic strategy by simultaneously increasing proteotoxic stress and preventing compensatory survival responses.

Several limitations should be considered. Although ivermectin was used to pharmacologically inhibit KPNA2-associated activity, more selective KPNA2-targeting approaches are required to further validate its therapeutic potential. In addition, while our findings demonstrate that KPNA2 regulates p52/RelB nuclear accumulation, whether this regulation involves direct interaction with NF-κB components or indirect signaling mechanisms remains to be determined. Nevertheless, our study establishes KPNA2 as a key regulator of non-canonical NF-κB-mediated autophagic adaptation, providing new insights into the molecular mechanisms governing BTZ sensitivity in MM.

Conclusion

In conclusion, this study uncovers a previously unidentified role of KPNA2 in regulating BTZ sensitivity in MM. We demonstrate that KPNA2 expression is progressively elevated during MM progression and is associated with unfavorable clinical outcomes. Functionally, KPNA2 enhances malignant behaviors and protects MM cells from BTZ-induced apoptosis. Mechanistically, KPNA2 activates the non-canonical NF-

κB pathway by promoting p52/RelB nuclear accumulation, which subsequently induces autophagic adaptation and enables myeloma cells to survive proteasome inhibition-induced stress. Genetic depletion or pharmacological inhibition of KPNA2 disrupts this signaling network, suppresses tumor growth, and restores BTZ sensitivity both *in vitro* and *in vivo*. These findings reveal KPNA2 as a critical molecular hub connecting nuclear transport, alternative NF-κB signaling, and autophagy-dependent proteostasis. Targeting the KPNA2/non-canonical NF-κB/autophagy axis represents a promising therapeutic strategy to enhance BTZ sensitivity and improve treatment outcomes for patients with MM.

Declarations

Funding

This study was supported by the National Natural Science Foundation of China (81960043, 82560722, 82360043), the Cooperation Project of Science and Technology plan of Jiangxi Province (20212BDH80024) and the Jiangxi Provincial Key Laboratory of Hematological Diseases (No. 2024SSY06051).

Availability of data and materials

The publicly available gene expression microarray datasets analyzed in this study were obtained from the Gene Expression Omnibus (GEO) repository under accession numbers GSE47552, GSE16122, GSE24080, and GSE136337. These datasets are freely accessible through the GEO database. Additional data supporting the findings of this study are available from the first author upon reasonable request.

Author contributions

FL and HW designed the research. HW, LZ, ZC, and MC performed the experiments and analyzed the data. HW and LZ collected clinical samples. HW and WZ wrote the manuscript. FL and LQ critically revised the manuscript. All authors read and approved the final manuscript.

Ethics approval and consent to participate

The study was approved by the Ethics Committee of the First Affiliated Hospital of Nanchang University. Informed consent was obtained according to the Declaration of Helsinki.

Acknowledgments

Not applicable.

Conflict of interest

All authors declare that they have no conflict of interest.

References

1. Kumar SK, Rajkumar V, Kyle RA et al (2017) Multiple myeloma. Nat Rev Dis Primers 3:17046. https://doi.org/10.1038/nrdp.2017.46
2. Davis LN, Sherbenow DW (2021) Emerging therapeutic strategies to overcome drug resistance in multiple myeloma. Cancers 13:1686. https://doi.org/10.3390/cancers13071686
3. Obeng EA, Carlson LM, Gutman DM et al (2006) Proteasome inhibitors induce a terminal unfolded protein response in multiple myeloma cells. Blood 107:4907–4916. https://doi.org/10.1182/blood-2005-08-3531
4. Niewerth D, Jansen G, Assaraf YG et al (2015) Molecular basis of resistance to proteasome inhibitors in hematological malignancies. Drug Resist Updat 18:18–35. https://doi.org/10.1016/j.drup.2014.12.001
5. Bashiri H, Tabatabaeian H (2023) Autophagy: A potential therapeutic target to tackle drug resistance in multiple myeloma. Int J Mol Sci 24:6019. https://doi.org/10.3390/ijms24076019
6. Desantis V, Saltarella I, Lamanuzzi A et al (2018) Autophagy: A new mechanism of prosurvival and drug resistance in multiple myeloma. Transl Oncol 11:1350–1357. https://doi.org/10.1016/j.tranon.2018.08.014
7. Debnath J, Gammoh N, Ryan KM (2023) Autophagy and autophagy-related pathways in cancer. Nat Rev Mol Cell Biol 24:560–575. https://doi.org/10.1038/s41580-023-00585-z
8. Xia J, He Y, Meng B et al (2020) NEK2 induces autophagy-mediated bortezomib resistance by stabilizing Beclin-1 in multiple myeloma. Mol Oncol 14:763–778. https://doi.org/10.1002/1878-0261.12641
9. Tang P, Yu Z, Sun H et al (2024) CRIP1 involves the pathogenesis of multiple myeloma via dual-regulation of proteasome and autophagy. EBioMedicine 100:104961. https://doi.org/10.1016/j.ebiom.2023.104961
10. Vogl DT, Stadtmauer EA, Tan K et al (2014) Combined autophagy and proteasome inhibition: a phase 1 trial of hydroxychloroquine and bortezomib in patients with relapsed/refractory myeloma. Autophagy 10:1380–1390. https://doi.org/10.4161/auto.29264
11. Harreman MT, Cohen PE, Hodel MR et al (2003) Characterization of the auto-inhibitory sequence within the N-terminal domain of importin alpha. J Biol Chem 278:21361–21369. https://doi.org/10.1074/jbc.M301114200
12. Han Y, Wang X (2020) The emerging roles of KPNA2 in cancer. Life Sci 241:117140. https://doi.org/10.1016/j.lfs.2019.117140
13. Sakai M, Sohda M, Miyazaki T et al (2010) Significance of karyopherin-alpha 2 (KPNA2) expression in esophageal squamous cell carcinoma. Anticancer Res 30:851–856
14. Wang CI, Wang CL, Wang CW et al (2011) Importin subunit alpha-2 is identified as a potential biomarker for non-small cell lung cancer by integration of the cancer cell secretome and tissue transcriptome. Int J Cancer 128:2364–2372. https://doi.org/10.1002/ijc.25568
15. Zheng M, Tang L, Huang L et al (2010) Overexpression of karyopherin-2 in epithelial ovarian cancer and correlation with poor prognosis. Obstet Gynecol 116:884–891.

https://doi.org/10.1097/AOG.0b013e3181f104ce

16. Cilloni D, Martinelli G, Messa F et al (2007) Nuclear factor κB as a target for new drug development in myeloid malignancies. Haematologica 92:1224–1229. https://doi.org/10.3324/haematol.11199
17. Vrábel D, Pour L, Ševčíková S (2019) The impact of NF-κB signaling on pathogenesis and current treatment strategies in multiple myeloma. Blood Rev 34:56–66. https://doi.org/10.1016/j.blre.2018.11.003
18. Demchenko YN, Glebov OK, Zingone A et al (2010) Classical and/or alternative NF-κB pathway activation in multiple myeloma. Blood 115:3541–3552. https://doi.org/10.1182/blood-2009-09-243535
19. Verzella D, Pescatore A, Capece D et al (2020) Life, death, and autophagy in cancer: NF-κB turns up everywhere. Cell Death Dis 11:210. https://doi.org/10.1038/s41419-020-2399-y
20. Trocoli A, Djavaheri-Mergny M (2011) The complex interplay between autophagy and NF-κB signaling pathways in cancer cells. Am J Cancer Res 1:629–649
21. Yi H, Liang L, Wang H et al (2021) Albendazole inhibits NF-κB signaling pathway to overcome tumor stemness and bortezomib resistance in multiple myeloma. Cancer Lett 520:307–320. https://doi.org/10.1016/j.canlet.2021.08.009
22. Wang C, Yu C, Huang Y et al (2018) Association of overexpressed karyopherin alpha 2 with poor survival and its contribution to interleukin-1β-induced matrix metalloproteinase expression in oral cancer. Head Neck 40:1719–1733. https://doi.org/10.1002/hed.25145
23. Rajkumar SV, Dimopoulos MA, Palumbo A et al (2014) International Myeloma Working Group updated criteria for the diagnosis of multiple myeloma. Lancet Oncol 15:e538–e548. https://doi.org/10.1016/S1470-2045(14)70442-5
24. Nakanishi A, Okumura H, Hashita T et al (2022) Ivermectin inhibits HBV entry into the nucleus by suppressing KPNA2. Viruses 14:2468. https://doi.org/10.3390/v14112468
25. Wagstaff KM, Sivakumaran H, Heaton SM et al (2012) Ivermectin is a specific inhibitor of importin alpha/beta-mediated nuclear import able to inhibit replication of HIV-1 and dengue virus. Biochem J 443:851–856. https://doi.org/10.1042/BJ20120150
26. van de Donk NCJ, Themeli M, Usmani SZ (2021) Determinants of response and mechanisms of resistance of CAR T-cell therapy in multiple myeloma. Blood Cancer Discov 2:302–318. https://doi.org/10.1158/2643-3230.BCD-20-0227
27. Steiner N, Ribatti D, Willenbacher W et al (2015) Marine compounds inhibit growth of multiple myeloma *in vitro* and *in vivo*. Oncotarget 6:8200–8209. https://doi.org/10.18632/oncotarget.3362
28. Ito S (2020) Proteasome inhibitors for the treatment of multiple myeloma. Cancers 12:265. https://doi.org/10.3390/cancers12020265
29. Narayanan S, Cai CY, Assaraf YG et al (2020) Targeting the ubiquitin-proteasome pathway to overcome anti-cancer drug resistance. Drug Resist Updat 48:100663. https://doi.org/10.1016/j.drup.2019.100663

30. Mogollón P, Díaz-Tejedor A, Algarín EM et al (2019) Biological background of resistance to current standards of care in multiple myeloma. Cells 8:1432. https://doi.org/10.3390/cells8111432
31. Lv J, Sun H, Gong L et al (2022) Aberrant metabolic processes promote the immunosuppressive microenvironment in multiple myeloma. Front Immunol 13:1077768. https://doi.org/10.3389/fimmu.2022.1077768
32. Hwang RD, Lu Y, Tang Q et al (2024) DBT is a metabolic switch for maintenance of proteostasis under proteasomal impairment. eLife 12:RP91002. https://doi.org/10.7554/eLife.91002
33. Amaravadi RK, Lippincott-Schwartz J, Yin XM et al (2011) Principles and current strategies for targeting autophagy for cancer treatment. Clin Cancer Res 17:654–666. https://doi.org/10.1158/1078-0432.CCR-10-2634
34. Yun Z, Zhichao J, Hao Y et al (2017) Targeting autophagy in multiple myeloma. Leuk Res 59:97–104. https://doi.org/10.1016/j.leukres.2017.06.002
35. Hoang B, Benavides A, Shi Y et al (2009) Effect of autophagy on multiple myeloma cell viability. Mol Cancer Ther 8:1974–1984. https://doi.org/10.1158/1535-7163.MCT-08-1177
36. Brownlie RJ, Kennedy R, Wilson EB et al (2023) Cytokine receptor IL27RA is an NF-κB-responsive gene involved in CD38 upregulation in multiple myeloma. Blood Adv 7:3874–3890. https://doi.org/10.1182/bloodadvances.2022009044
37. Fabre C, Mimura N, Bobb K et al (2012) Dual inhibition of canonical and noncanonical NF-κB pathways demonstrates significant antitumor activities in multiple myeloma. Clin Cancer Res 18:4669–4681. https://doi.org/10.1158/1078-0432.CCR-12-0779

Figures

Figure 1

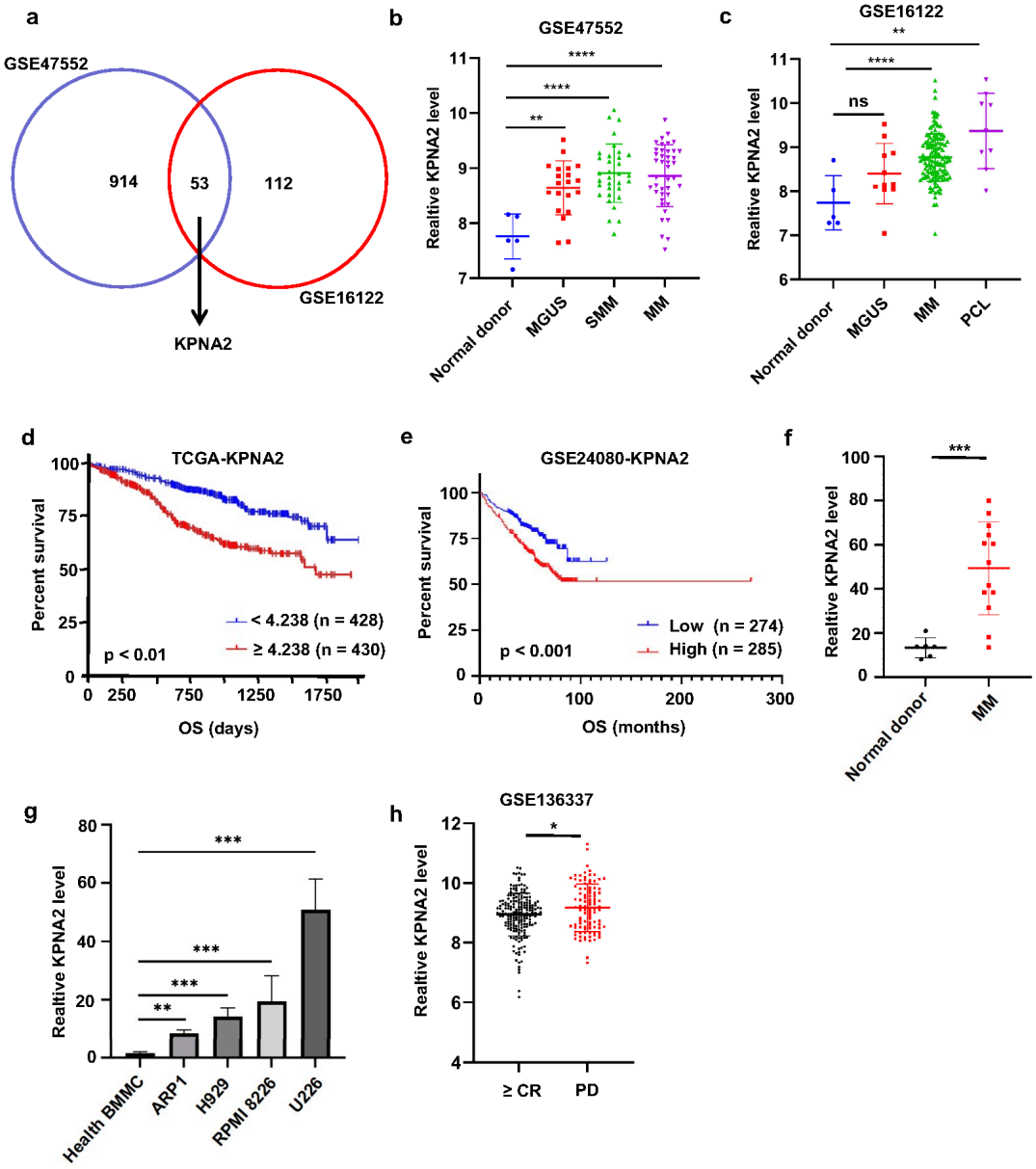


Figure 1

High-level KPNA2 is associated with poor outcome in patients with MM

(A) Venn diagram showing 53 overlapping DEGs, including KPNA2, between the GSE47552 and GSE16122 datasets. **(B)** KPNA2 mRNA expression was significantly upregulated in MGUS (n = 20), SMM (n = 33), and MM (n = 41) compared with healthy donors (n = 5) in GSE47552 (**$p < 0.01$, ***$p < 0.001$).

(C) In GSE16122, KPNA2 levels were markedly elevated in MM (n = 133) and PCL (n = 9) vs. healthy donors (n = 5) (ns, no significance; $^{**}p < 0.01$, $^{***}p < 0.001$). **(D)** Kaplan–Meier analysis of 858 TCGA MM patients showed shorter OS in the high KPNA2 group (n = 430) than in the low group (n = 428, $^{**}p < 0.01$). **(E)** Kaplan–Meier analysis of the GSE24080cohort confirmed poorer OS in patients with high KPNA2 expression (n = 285 vs. 274, $^{***}p < 0.001$). **(F)** RT–qPCR results verified increased KPNA2 mRNA expression in NDMM patient bone marrow plasma cells (n = 13) relative to healthy controls (n = 6) ($^{***}p < 0.001$). **(G)** Compared with healthy BMMCs, elevated KPNA2 mRNA expression was detected in MM cell lines (ARP1, H929, RPMI 8226, U266; $^{**}p < 0.01$, $^{***}p < 0.001$). **(H)** In BTZ-treated MM patients (GSE136337), KPNA2 expression was higher in cases with progressive disease (PD) (n = 99) than in those achieving complete response or better (≥ CR) (n = 194) ($^{*}p < 0.05$).

Figure 2

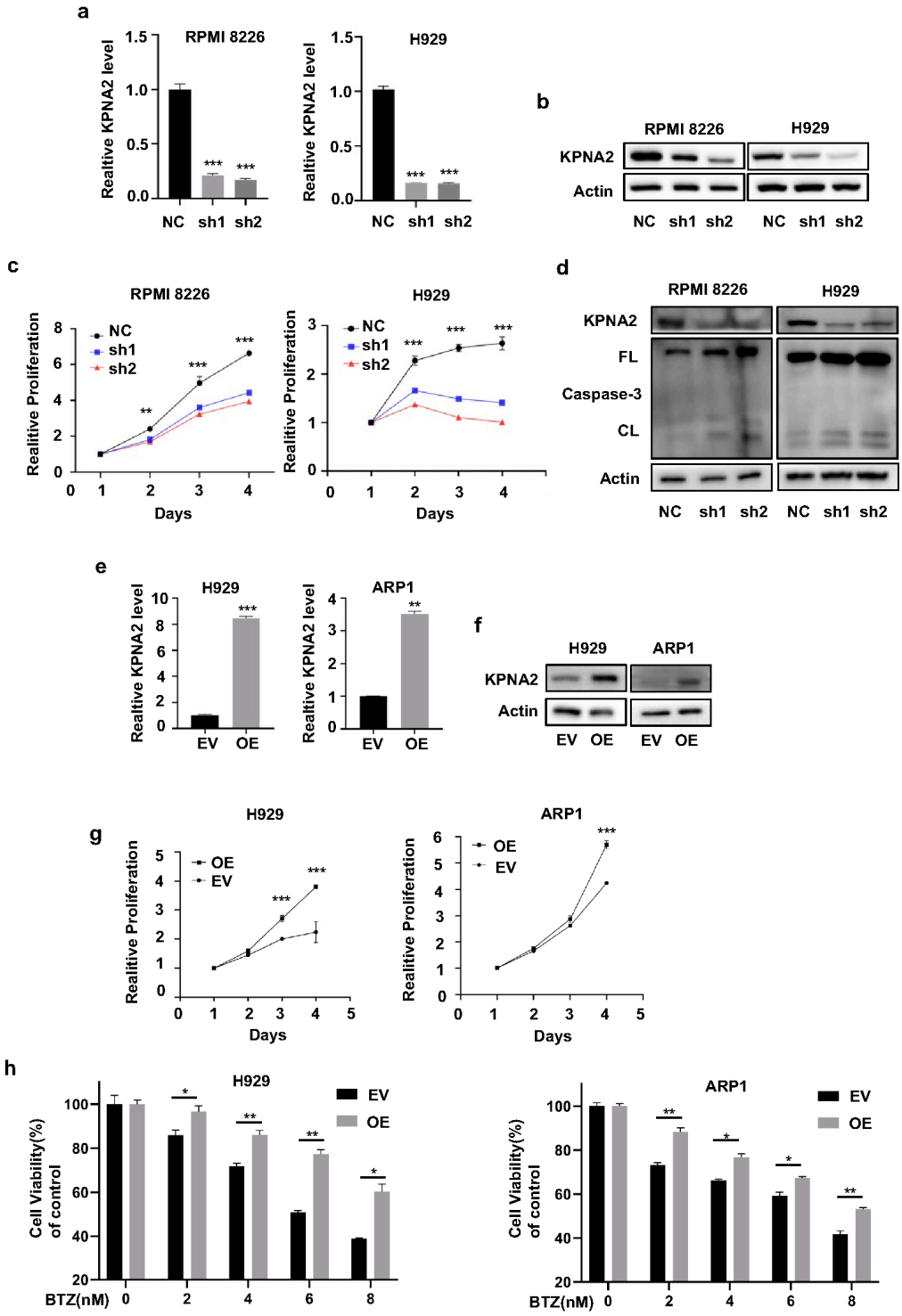


Figure 2

KPNA2 promotes malignant progression and attenuates BTZ sensitivity in MM cells

(A-B) RT-qPCR and Western blot analyses confirmed significant downregulation of KPNA2 mRNA and protein in KPNA2-sh1/sh2 RPMI 8226 and H929 cells relative to NC cells (***p < 0.001). **(C)** KPNA2 knockdown markedly suppressed cell viability in MM cell lines (**p < 0.01, ***p < 0.001). **(D)** Knockdown

of KPNA2 upregulated the protein levels of apoptotic markers cleaved caspase-3. **(E-F)** RT-qPCR and Western blot assays verified significant upregulation of KPNA2 mRNA and protein in KPNA2-overexpressing (OE) H929 and ARP1 cells compared with empty vector (EV) controls (**p < 0.01, ***p < 0.001). **(G)** KPNA2 overexpression significantly promoted cell viability in H929 and ARP1 cells (****p* < 0.001). **(H)** CCK–8 assays were performed to detect cell proliferation in H929-EV, H929-KPNA2-OE, ARP1-EV, and ARP1-KPNA2-OE cells after 24 h of treatment with 0-8 nM bortezomib (BTZ). KPNA2-OE cells exhibited significantly higher proliferative activity than control cells (**p* < 0.05, ***p* < 0.01).

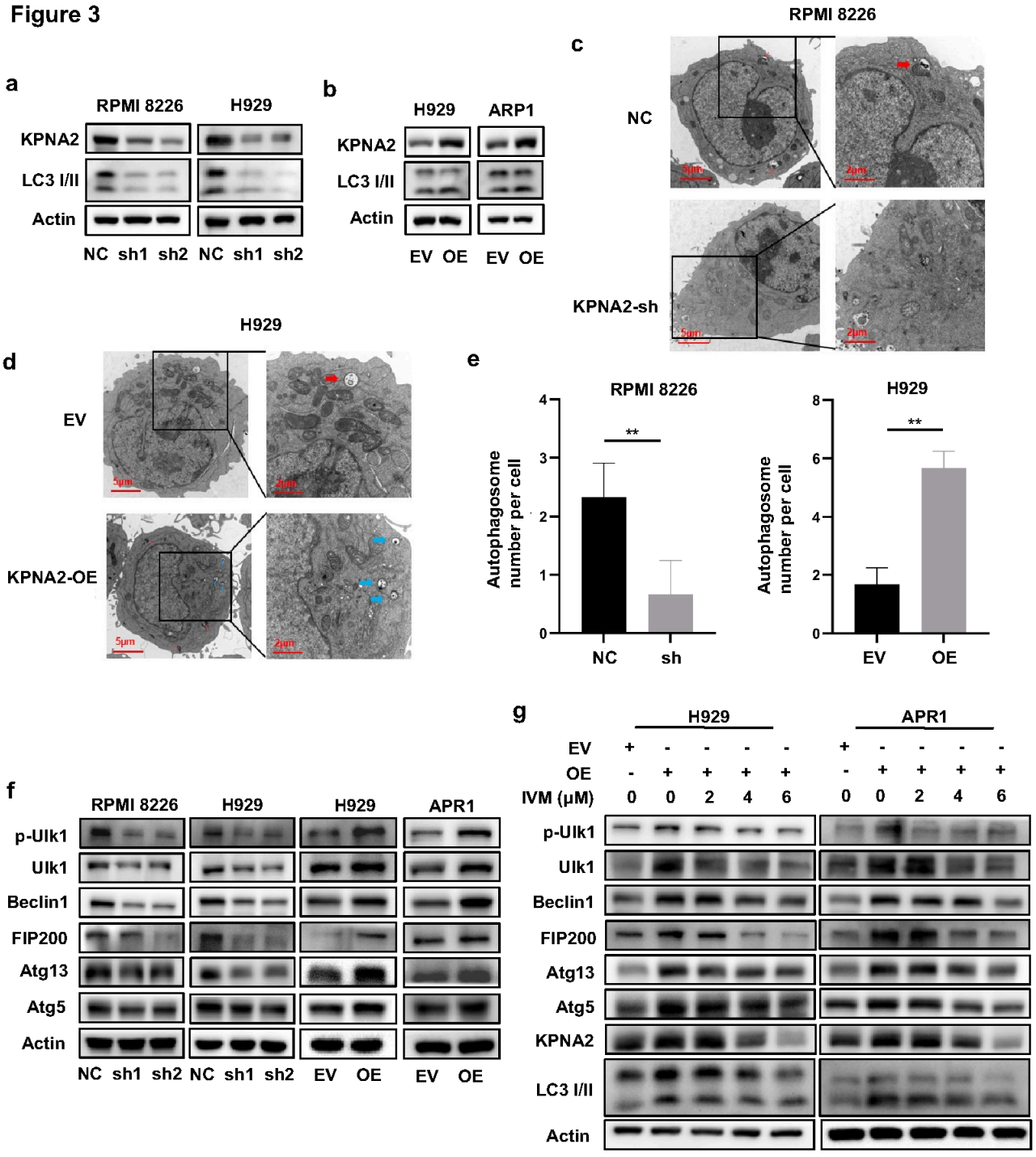


Figure 3

KPNA2 activates autophagy in MM cells

(A) Western blot showed reduced LC3 II levels in KPNA2-knockdown RPMI 8226 and H929 cells. **(B)** KPNA2 overexpression upregulated LC3 II protein expression in H929 and ARP1 cells. **(C)** TEM imaging revealed fewer autolysosomes (red arrows) in KPNA2-deficient RPMI 8226 cells relative to controls. **(D)** Increased autophagosome abundance (blue arrows) was observed in KPNA2-overexpressing H929 cells via TEM analysis. **(E)** Statistical quantification of autophagosomes and autolysosomes in TEM images (**$p < 0.01$). **(F)** KPNA2 knockdown decreased the levels of core autophagic proteins (FIP200, p-ULK1, ULK1, ATG13, ATG5, Beclin1) in RPMI 8226 and H929 cells. KPNA2 overexpression elevated the expression of these autophagy-associated proteins in H929 and ARP1 cells. **(G)** Gradient IVM treatment (0-6 μM, 24 h) downregulated autophagic protein levels (FIP200, p-ULK1, ULK1, ATG13, ATG5, LC3 II, Beclin1) in KPNA2-overexpressing MM cells.

Figure 4

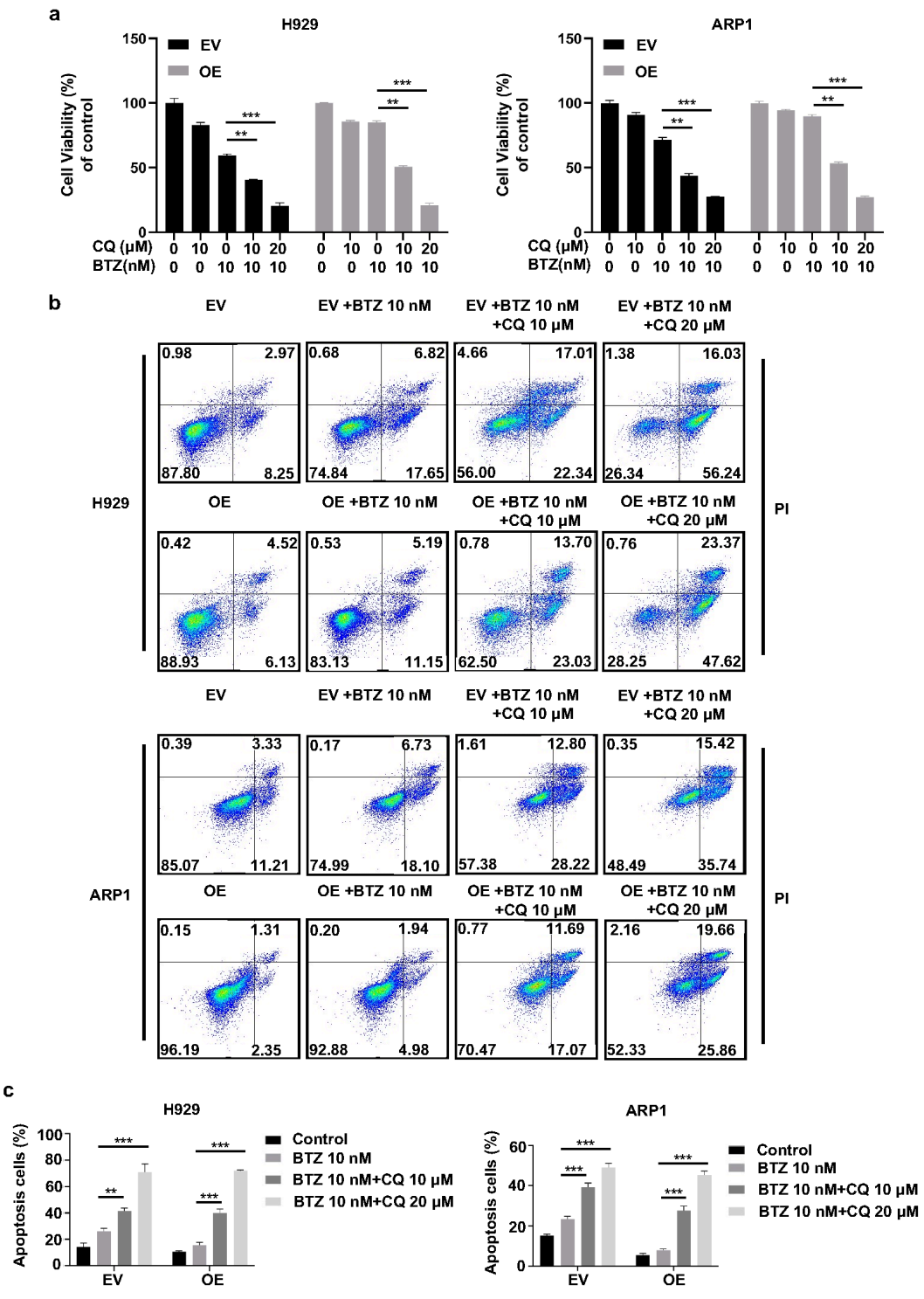


Figure 4

KPNA2- mediated autophagic stress adaptation is associated withdecreased sensitivity to BTZ

(A) CCK–8 assays showed that combined treatment with CQ (0, 10, 20 μM) and 10 nM BTZ for 24 h significantly reduced MM cell viability compared with BTZ monotherapy (**$p < 0.01$, ***$p < 0.001$). **(B)** Flow cytometry demonstrated enhanced cell apoptosis following combined CQ and BTZ treatment

relative to BTZ monotherapy. **(C)**Statistical summary of flow cytometry apoptosis results (**$p < 0.01$, ***$p < 0.001$).

Figure 5

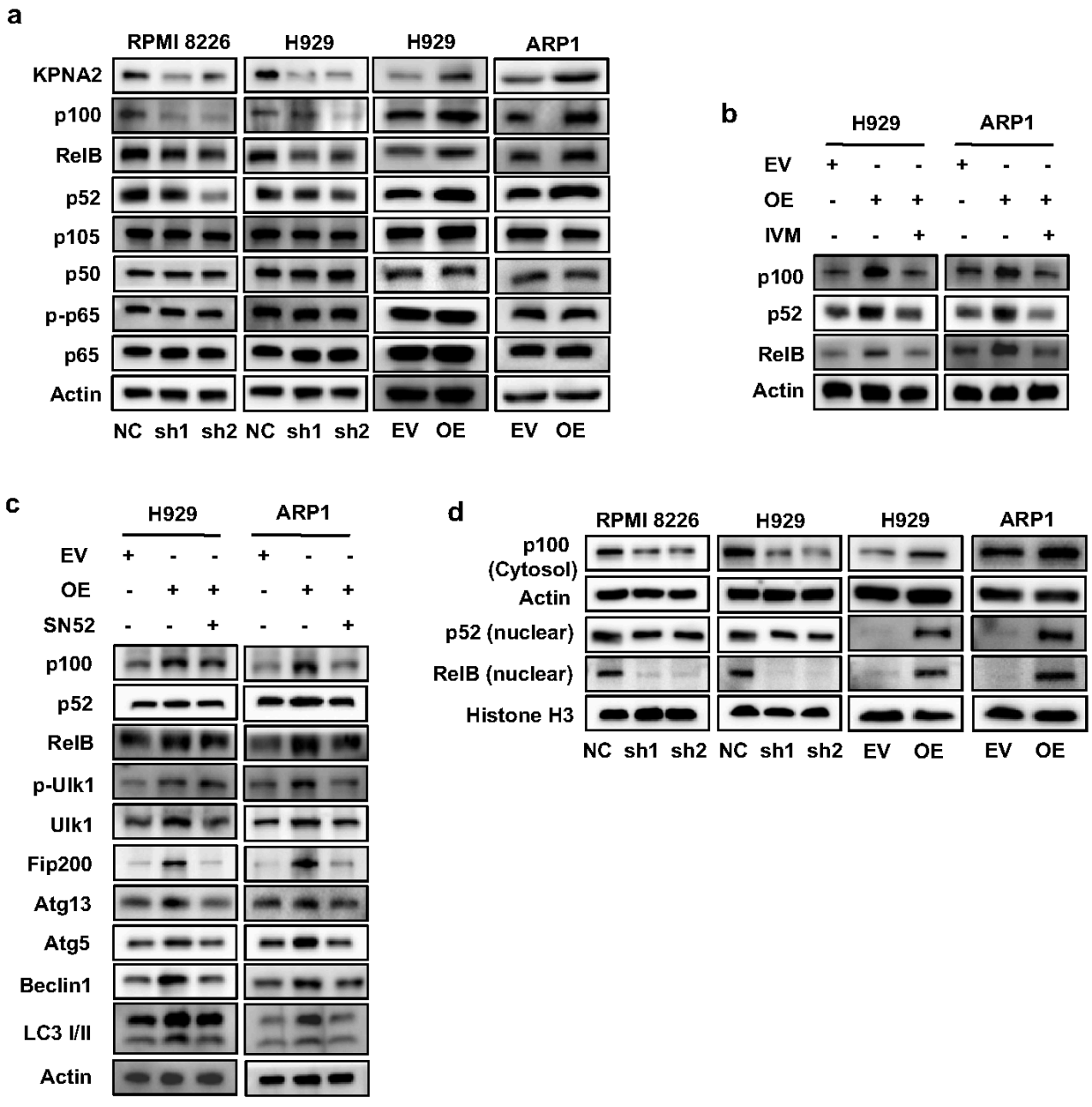


Figure 5

KPNA2 activates autophagy through non-classic NF-κB signaling pathway in MM cells

(A) In KPNA2-knockdown RPMI 8226 and H929 cells, canonical NF-κB markers (p65, p-p65, p105, p50) remained unaltered, while non-canonical NF-κB proteins (p100, p52, RelB) were downregulated. In KPNA2-overexpressing H929 and ARP1 cells, canonical NF-κB expression showed no obvious changes, whereas non-canonical NF-κB markers (p100, p52, RelB) were significantly upregulated. **(B)** Treatment with 5 μM IVM for 24 h markedly decreased non-canonical NF-κB protein levels (p100, p52, RelB) in KPNA2-overexpressing MM cells. **(C)** After 24 h of treatment with 15 μM SN52, KPNA2-overexpressing cells exhibited reduced expression of both autophagy-related proteins (FIP200, p-ULK1, ULK1, ATG13, ATG5, LC3 II, Beclin1) and non-canonical NF-κB markers (p100, p52, RelB). **(D)** KPNA2 knockdown decreased cytoplasmic p100 and nuclear p52/RelB levels in RPMI 8226 and H929 cells. KPNA2 overexpression increased cytoplasmic p100 and nuclear p52/RelB abundance in H929 and ARP1 cells.

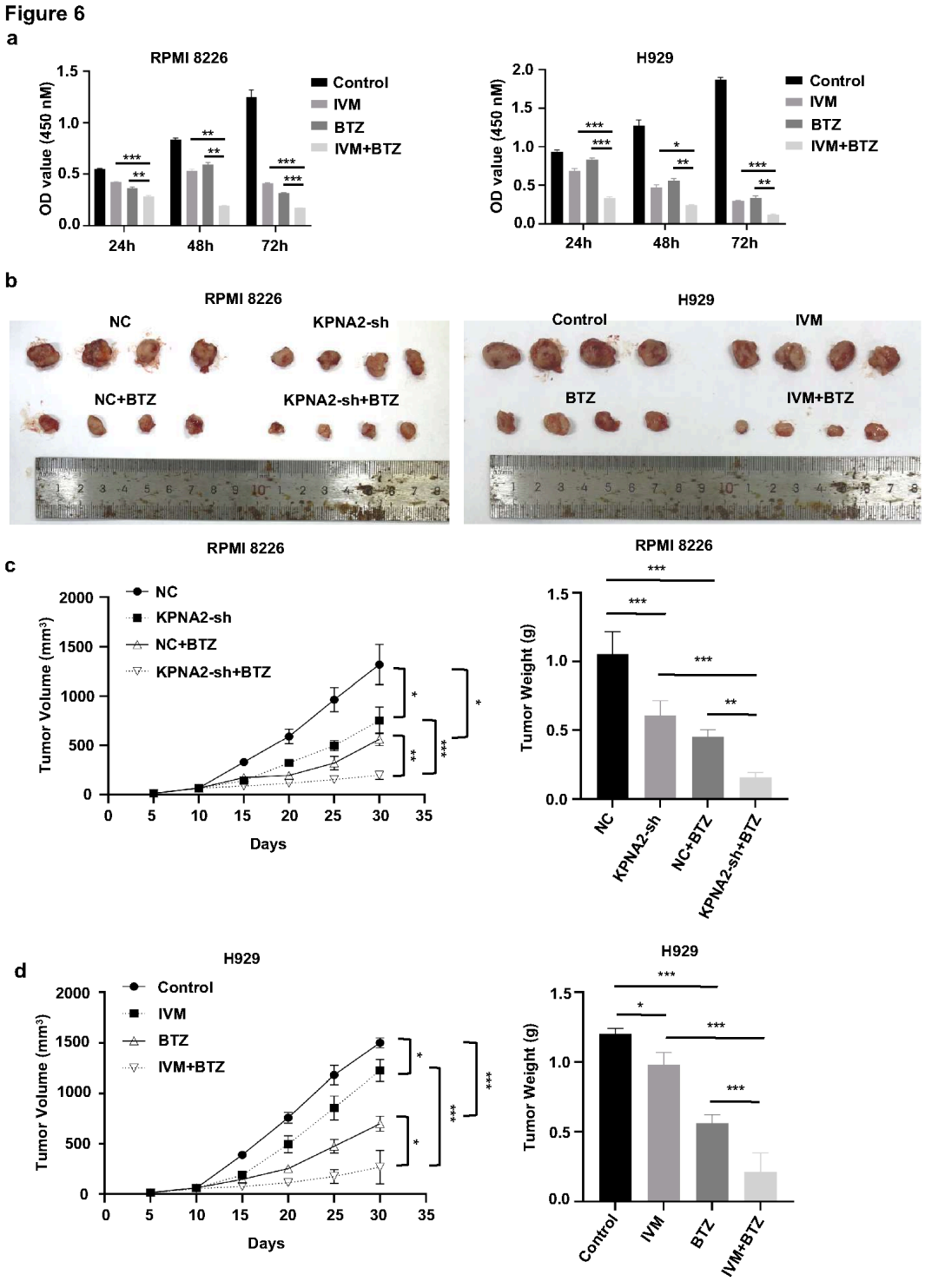


Figure 6

KPNA2 inhibition potentiates the antimyeloma effects of BTZ *in vitro*and *in vivo*

(A) RPMI 8226 and H929 cells were treated with 5 μM IVM and 10 nM BTZ alone or in combination for 24 h, 48 h, and 72 h, respectively. Cell proliferation was detected by the CCK–8 assay. Compared with the group treated with IVM or BTZ alone, the combined treatment group showed a more significant inhibition

of cell proliferation (***$p < 0.001$, **$p < 0.01$, *$p < 0.05$). **(B)** Tumors from each treatment group were excised and photographed; the group treated with BTZ combined with KPNA2 inhibition showed the smallest tumor volume. **(C-D)** Changes in tumor volume of each group were detected and recorded to plot tumor growth curves. Compared with the single-treatment groups, the RPMI 8226 KPNA2-sh + BTZ group and H929 + IVM + BTZ group had the smallest tumor volumes (*$p< 0.05$, **$p < 0.01$, ***$p < 0.001$). Tumors from each group were excised and weighed after 30 days, and statistical analysis was performed on the tumor weights. Compared with the single-treatment groups, the RPMI 8226 KPNA2-sh + BTZ group and H929 + IVM + BTZ group had the lightest tumor weights (*$p < 0.05$, **$p < 0.01$, ***$p < 0.001$).

Supplementary Files

This is a list of supplementary files associated with this preprint. Click to download.

- Supplementaryfigureslegend.docx
- Supplementaryfigures.pdf
- Supplementarytable.docx
- WesternBlotorginblots.pdf